



Size Fractionation of Milliliter DNA Samples in Minutes Controlled by an Electric Field of ~ 10 V

Paul Bruand, Inga Tijunelyte, Adrien Castinel, Cécile Donnadiou, Pierre Joseph,
Aurélien Bancaud

► To cite this version:

Paul Bruand, Inga Tijunelyte, Adrien Castinel, Cécile Donnadiou, Pierre Joseph, et al.. Size Fractionation of Milliliter DNA Samples in Minutes Controlled by an Electric Field of ~ 10 V. *Analytical Chemistry*, 2023, 95 (49), pp.18099-18106. <10.1021/acs.analchem.3c03187>. <hal-04322873>

HAL Id: hal-04322873

<https://laas.hal.science/hal-04322873v1>

Submitted on 5 Dec 2023

HAL is a multi-disciplinary open access archive for the deposit and dissemination of scientific research documents, whether they are published or not. The documents may come from teaching and research institutions in France or abroad, or from public or private research centers.

L'archive ouverte pluridisciplinaire **HAL**, est destinée au dépôt et à la diffusion de documents scientifiques de niveau recherche, publiés ou non, émanant des établissements d'enseignement et de recherche français ou étrangers, des laboratoires publics ou privés.



HAL Authorization

SIZE-FRACTIONATION OF MILLI-LITER DNA SAMPLES IN MINUTES CONTROLLED BY AN ELECTRIC FIELD OF ~10 V

Paul Bruand^{1,2}, Inga Tijunelyte¹, Adrien Castinel³, Cécile Donnadiou³, Pierre Joseph¹, Aurélien Bancaud^{1,*}

¹*CNRS, LAAS, 7 avenue du colonel Roche, F-31400, Toulouse, France.*

²*Adelis, 478 Rue de la Découverte, 31670 Labège, France*

³*GeT-PlaGe, US 1426, Genotoul, INRAE, 31320 Castanet-Tolosan, France*

Correspondence should be sent to Aurélien BANCAUD (abancaud@laas.fr, +33 5 61 33 62 46)

Abstract (196 words)

DNA size fractionation is an essential tool in molecular biology, which is used to isolate targets in a mixture characterized by a broad molecular weight (MW) distribution. Microfluidics was thought to provide opportunity to create devices capable of enhancing and speeding up the classical fractionation processes. However, this conjecture met limited success due to the low mass and/or volume throughput of these technologies. We describe the μ LAF (μ Laboratory for DNA Fractionation) technology for DNA size selection based on the stacking of molecules on films of $\sim 100\ \mu\text{m}$ in thickness with 10^5 pores of $\sim 2\ \mu\text{m}$ in diameter. Size selection is achieved by controlling the regime of electrohydrodynamic migration in the pores through the temporal modulation of an electric field. This technology allows the processing of milliliter-scale samples containing a DNA mass of several hundreds of ng within ~ 10 minutes, and the selection of DNA in virtually any size window spanning 200 to 1000 bp. We demonstrate that one operation suffices to fractionate sheared genomic DNA in up to six fractions with collection efficiencies of $\sim 20\text{-}40\%$ and enrichment factors of $\sim 1.5\text{-}3$ fold. These performances compare favorably in terms of speed and versatility to those of current standards.

Introduction

The purification and size fractionation of nucleic acids from biological specimens enables the production of processable material for subsequent analysis, including, to cite but a few, sequencing or cloning^{1,2}. Band excision after separation by slab gel electrophoresis has been the initial standard³, but this technique takes a long time and requires several extraction, centrifugation, washing and precipitation steps that makes it labor-intensive. Even automatized with dedicated cartridges⁴, this technology lasts one to several hours for low and high MW molecules, respectively. To address some of these shortcomings, solid-phase extraction, in which DNA is reversibly bound to silica particles, washed, and then eluted^{5,6}, has been implemented. Size selection can be achieved using solid phase extraction methods because the increase of the adsorption energy with the size of the molecules enables high MW selection by competitive interaction. This operation requires the accurate control of the DNA-to-particle concentration ratio in order to obtain a tunable cut-off in the range of 150 to 700 bp⁷. Fractionation is then attained by repeating two rounds of extraction with different size selection that enable removal of the low- and high-MW fractions of the sample. Using magnetic beads for particle handling rather than centrifugation⁸, parallelization, and automatization can be achieved, although the number of washing steps remains an issue to speed up the process.

Microfluidic technologies have been vaunted as unique solutions for the fractionation of DNA. Pioneering studies used a high-performance of capillary electrophoresis system coupled to a fraction collector in order to isolate up to 60 fractions with excellent base-pair resolution⁹⁻¹¹. This approach is however intrinsically limited by the low volume and limited DNA mass in each collected fraction due to the internal volume of capillaries and the risk of saturation during the separation, respectively. Massive parallelization and optimization of the collection outlet¹² with microfabrication technologies were thought to overcome these limitations. Yet, beyond proof-of-principle experiments^{13,14}, the processed mass has not, to the best of our knowledge, been enhanced to the level of tens ng in microfluidic chips. Instead of loading an initial mass of the sample in a separation channel, it has been proposed to separate DNA in space in order to continuously collect a fraction defined by its position. The technique of continuous flow separation has been shown to enhance the sample throughput and facilitate the sample recovery. Different separation matrices have been tested using conventional polymer gels¹⁵, or artificial matrices made out of periodic pillar arrays¹⁶, and slanted nanofilter arrays¹⁷. Best performances were reported for high MW molecules, but the requirement for sophisticated and costly fabrication techniques still represents an issue in comparison to silica particles. Moreover, the

concentration of the fractionated sample remains low at the outlet, because the separation process is inherently associated to an onset in dilution due to band broadening. Consequently, microfluidic technologies have not yet met the needs of DNA fractionation for applications in genomics.

We recently developed the “ μ -Laboratory for DNA Analysis and Separation” (μ LAS) technology for DNA separation and concentration within the size range of 0.1 to 200 kbp^{18,19}. μ LAS is operated by simultaneously controlling a viscoelastic flow and a counter electrophoretic force for the convection of DNA along microchannels. Electrohydrodynamic migration is also associated a transverse viscoelastic migration oriented towards the channel walls²⁰. Note that this transverse force also occurs in Newtonian fluids for high MW molecules of ~ 50 kbp^{21,22}, but the amplitude of these transverse migration forces is insufficient for the processing of molecules of less than 1 kbp¹⁹. Transverse viscoelastic forces increase with the size of DNA, so that high MW molecules migrate near the walls along low-velocity field lines, whereas smaller ones travel faster closer to the channel centerline. This property can be exploited to perform DNA separation in a linear channel, but also the operations of concentration, purification, biosensing, and/or size selection using a funnel-shaped channel^{20,23,24}. So far, however, we could only obtain a size selection threshold for high MW DNA in the range of 5 to 40 kbp, and we were limited in mass throughput below 10 ng²⁵. These inadequate performances, which were explained by the aggregation of DNA molecules and their uncontrolled migration in capillaries²⁵, prompted us to design a new format, hereafter termed μ LAF (“ μ -Laboratory for DNA Fractionation”), to process milli-Liter samples containing hundreds of ng with a tunable threshold in the conventional range of 200 to 1000 bp. In the following, we introduce and describe μ LAF, then demonstrate the optimization of its operation with molecular biology size standards before fractionating sheared genomic DNA samples in up to 6 consecutive fractions in one round of operation.

Experimental

Reagents, buffer, and disposable material

Molecular biology grade chemicals were purchased from Sigma-Aldrich. DNA ladder solutions were composed of a DNA 100 bp ladder (ThermoFisher Scientific) and single bands of 500 bp. We also used bovine genomic DNA (genome ref: ARS-UCD (bausTau9), 3 Gbp), which was extracted using Gentra Puregene Tissue Qiagen method (Qiagen, cat# 158667). We collected 4.2 μ g in 20 μ L, and the sample was characterized

by a bimodal size distribution of 700 and 15,000 bp, as inferred from electrophoretic separation with the Fragment Analyzer (Supplementary Fig. S1A). This material was then fragmented by sonication on a Covaris M220 (Covaris, cat# 500295). Following the recommendations of the supplier, we used 200 ng diluted in 54 μ L of TE (Tris-HCl, 10 mM, EDTA, 1 mM pH=7), and applied the following set of parameters (Duty factor: 20%; Peak Incident Power: 50W; Cycles per burst: 200; Duration: 45 s; Temperature: 20°C). The peak of the broad size distribution was ~800 bp (Supplementary Fig. S1B).

For μ LAF process, the running buffer consisted of 15 mM Bis-Tris, 5 mM PIPES, 0.5 mM EDTA, and 5% (w:v) 360 kDa PVP (Polyvinylpyrrolidone). The viscosity of this solution, filtered at 0.8 μ m before use, was 42 mPa.s, as measured from the average velocity of the solution for a given pressure using a plug of fluorescent dye as reporter (Agilent Capillary Electrophoresis). The electrical conductivity was 500 μ S/cm using a portable conductivity meter (Mettler Toledo).

Isoporous Ion track-etched films made of Polycarbonate were purchased from it4ip (Belgium). They are obtained by irradiating thin polymer films with energetic particles so as to form latent tracks that are converted into regular pores by a chemical treatment. Their characteristics in pore radius R , thickness L , and pore density D were: (i) $R=2.5 \mu\text{m}$, $L=46 \mu\text{m}$, $D=10^5 \text{ cm}^{-2}$; (ii) $R=1 \mu\text{m}$, $L=23 \mu\text{m}$, $D=4 \cdot 10^5 \text{ cm}^{-2}$; (iii) $R=1 \mu\text{m}$, $L=48 \mu\text{m}$, $D=4 \cdot 10^5 \text{ cm}^{-2}$; (iv) $R=1 \mu\text{m}$, $L=123 \mu\text{m}$, $D=10^5 \text{ cm}^{-2}$.

3D device and instrumentation

The fluidic device was fabricated using a 3D stereolithography printer (DWS Digitalwax 029 J+) and an acrylic biocompatible resist (DWS DS3000). The opening for the isopore film was 1 cm^2 . Platinum electrodes grids with a mesh size of 500 μm (open surface 0.6 cm^2 , total surface 1 cm^2) and a thickness of 400 μm (Auray Laser, France) were incorporated in the fluidic device to monitor the electric field. Both electrodes were placed at 2 mm from the film. The total volume enclosed between the two electrodes was 450 μL .

Solutions were injected in the device at a constant pressure delivered by a pressure controller (Fluigent Flow EZ TM, 7 bar). The running buffer or DNA solution could alternatively be injected by means of a 3-port/2-way sampling valve (Fluigent 2-SWITCHTM). The electric field was applied with a DC power supply operated in the range of 4 to 12 V, and the current was monitored by a multimeter controlled with a LabVIEW program.

The electric field and hydrodynamic speed were deduced from the measured current and flow rate, respectively (see Supplementary Material).

DNA characterization

DNA solutions were collected in several fractions during the retention and release modes. These fractions were then weighed and subjected to quantification and/or size profiling using Qubit and BIABooster, respectively. For the quantitation of DNA samples, a Qubit dsDNA HS (high sensitivity, 0.1 to 120 ng) Assay Kit was used with a Qubit 4.0 fluorometer (Thermo Fisher Scientific) according to the manufacturer's protocols. Briefly, 10 μL of a Qubit standard was added to 190 μL of Qubit working solution for calibration, and 5 μL of the DNA sample was added to 195 μL of Qubit working solution. All prepared solutions were vortexed and incubated for 5 min before measurement. To estimate the total mass of DNA injected and retrieved during the experiment, we multiplied the measured DNA concentrations by the mass of the collected fractions. The typical error in the DNA mass measurements was 5% due to the weight variability of the Eppendorf tubes used for fraction collection. The concentration and size distribution analysis of DNA samples were conducted using the BIABooster system (Adelis). The BIABooster is a capillary electrophoresis plug-in system integrated with an Agilent 1600CE system. The detection module includes an ultra-sensitive laser-induced fluorescence (LIF) detector (Zetlif Laser (Adelis)) which has a limit of detection of 10 fg/ μL ¹⁸. DNA size and concentration of the samples were determined with the BIABooster Analytics software (Adelis) using the signal of a DNA ladder to convert the fluorescence intensity into DNA concentration, and migration time into base pairs.

Principle of the μLAF module

The μLAF technology is based on the switch between two regimes of migration dominated by hydrodynamic and electrophoresis in the macroscopic chamber upstream of the film *vs.* in the narrow pores of the film, respectively (left panel of Fig. 1A). This transition is associated with a reversion of the direction of migration, implying that molecules accumulate at the entry of the pore. Upon arrest of the electric field, stacked molecules are released from the pore (right panel of Fig. 1A). In the following, we propose to specify an instrument that concentrates milliliter DNA samples in minutes (e.g., at a flow rate of $\sim 300 \mu\text{L}/\text{min}$) based on

an array of pores etched in thin polymer films. From previous reports²⁰, we know that the conditions to concentrate DNA molecules in a pore of radius $R \sim 1 \mu\text{m}$ are characterized by a mean flow velocity v_0 of $\sim 1 \text{ mm/s}$ (the corresponding flow rate F_R is $\sim 2 \cdot 10^{-4} \mu\text{L/min}$) and an electric field E of $\sim 1 \text{ kV/cm}$. Taking an actuation tension of 10 V as delivered by a standard DC power supply, we estimate the film thickness L to be $\sim 100 \mu\text{m}$. The hydraulic resistance of the corresponding pore is $8 \cdot 10^{18} \text{ Pa.s/m}^3$, and $\sim 10^5$ pores are required to match the specified flow rate of $300 \mu\text{L/min}$ using the actuation pressure of 10^5 Pa (Fig. 1B). The section of the film is 1 cm^2 , implying that the expected pore density is 10^5 pore/cm^2 . The 3D-printed device should also contain two platinum grid-like electrodes with a mesh size of $500 \mu\text{m}$. The distance from the film is set to 2 mm (see supplementary material for electric field description), and the electric and hydrodynamic resistances in the volume separating the electrode and the film are 20-fold and 1000-fold lower than that of the film, respectively. Given the conductivity of the running buffer of $400 \mu\text{S/cm}$, the total electrical current in the system is $\sim 1 \text{ mA}$ (i.e., 10 nA per pore) at 10 V . Joule heating occurs in the pore just for a brief time interval on the order of $L/v_0 \sim 0.1 \text{ s}$, resulting in a modest onset in temperature in the pore of $\sim 0.05^\circ\text{C}$.

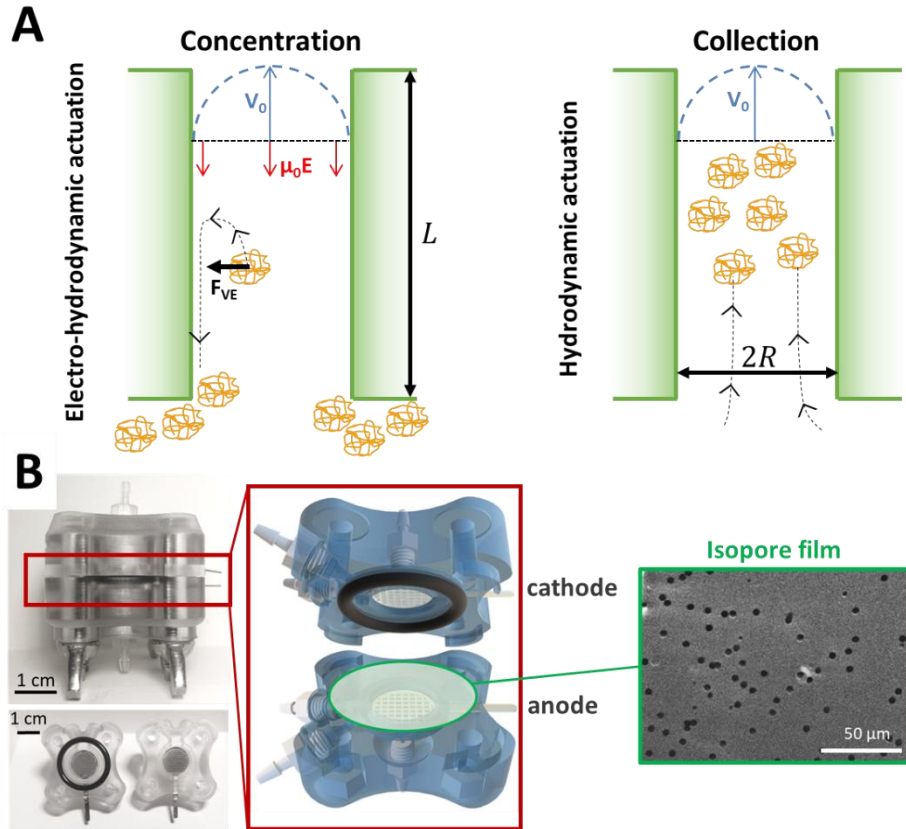


Figure 1 : Principle and design of μLAF . (A) The left panel shows the concentration of DNA using electrohydrodynamic actuation at the level of a single pore. The transverse viscoelastic force F_{VE} enables the transition from a hydrodynamic-dominated migration regime ahead of the pore to an electrophoresis-dominated regime inside the pore. The molecules

thus travel backward, as schematized by the dashed trajectory. Upon releasing the electric field (right panel), they can be collected downstream of the pore, i.e., towards the top of the figure. (B) μ LAF consists of an array of pores etched in a polymer film (electron micrograph with a green contour) and integrated in a 3D-printed device with two electrodes positioned 2 mm away from the film.

Results

Operation of μ LAF and optimization of the film geometry

The operation of the μ LAF system consisted of three consecutive steps of sample loading, stacking and rinsing, followed by collection (denoted 1, 2, and 3 in the inset of Fig. 2A). We started with a DNA solution containing one single DNA fragment of 500 bp diluted at the concentration of 0.3 ng/ μ L in the running buffer. Using a device initially filled with buffer, we injected a volume of 1.25 mL of DNA solution at a flow rate of 250 μ L/min, *i.e.*, the processed DNA mass was \sim 380 ng. As a reference experiment, the sample was processed without electric actuation (blue curve in Fig. 2A) by collecting 23 fractions at the outlet of μ LAF, and measuring their concentration (see methods). The signal appeared as a Heaviside function distorted by the passage through a dispersive system, which readily arises from Taylor dispersion. The same experiment was then operated with electrohydrodynamic actuation applying an electric field of 740 V/cm within the pores, which was generated by a power supply set to 10 V (red curve in Fig. 2A). Upon release of the electric field, we detected a peak of DNA with the enrichment factor of 3.9-fold. This enrichment was readily explained by the difference between the injection time of 300 s and the collection time of \sim 45 s, as inferred from the full width at half maximum of the collected peak. Later qualitative prediction associated with an enrichment factor of 6.7-fold is however greater than the experimental readout. This difference nevertheless was explained by the leak during the concentration phase, which corresponded to 105 \pm 5 ng, as measured by integrating the concentration signal before the release of the electric field. The total mass of DNA gathered after releasing the electric field was 235 \pm 12 ng (*i.e.*, 69 \pm 7% of the loaded sample). In the four most concentrated fractions, we collected 190 \pm 10 ng, or equivalently 48 \pm 5% of the initial sample, in a volume of 193 μ L, which is 6.5-fold lower than that of the injection. Therefore, the μ LAF platform enables the concentration and collection of milli-liter scale DNA samples using an electric field actuation of 10 V only.

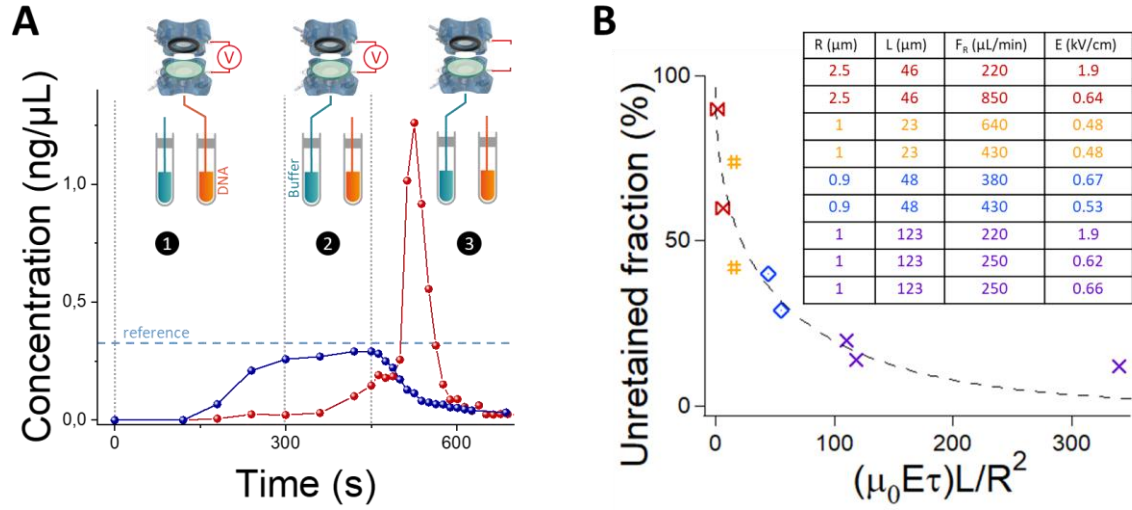


Figure 2: μ LAF operation and film optimization. (A) The graph reports the concentration of the fractions collected during the operation of the μ LAF system as a function of time. The process involves three steps of loading (1), rinsing (2), and collecting (3), which are separated by the vertical dashed lines in the plot. The red dataset is obtained using electric actuation, whereas the blue one corresponds to the reference without application of the electric field. The light blue vertical line is the concentration of the sample loaded in the system. (B) The leak fraction for four different film geometries indicated with red, yellow, blue, and purple colors and different actuation conditions (see the list in the table) is plotted as a function of the ratio of the transverse to longitudinal migration time (see the model in Supplementary Material). Note that τ is the viscoelastic fluid relaxation time and $\mu_0 E$ the electrophoretic velocity. In the table, F_R is the flow rate and E is the electric field. The dashed line corresponds to the prediction of the model.

The detection of a leak during the retention phase prompted us to investigate its origin in order to minimize its consequences. We used four different films with pore radii R of 2.5 or 1 μm and a length L in the range of 23, to 123 μm (see details in the Methods section). For each film, we performed two to three experiments using different electrohydrodynamic actuation settings, as specified in the inset of Fig. 2B. During the 4 min of stacking, we collected the solution at the outlet of the device and measured the mass of DNA it contained. Normalizing the results to the total amount of DNA, we obtained the proportion of unretained molecules, which spanned 12 to 90% (graph in Fig. 2B). This study showed that large pores of 2.5 μm in radius or short pores of 23 μm in length did not produce good systems for DNA processing due to the excessive leak of more than 45%. Furthermore, the films with a high thickness-to-radius aspect ratio allowed us to keep the leak fraction below 30%. We compared this data with a kinetic model based on the initial radial position of the molecule r_i and its migration in the pore as a result of transverse and longitudinal hydrodynamic drag forces (see details in Supplementary Material). We assumed that molecules were retained if they reached the wall of the pore, equivalently the backward electrophoresis-dominated migration regime, before exiting from this confined channel. We derived the critical radius R^* above which molecules were sufficiently close to the wall

for their stacking. Conversely, electrohydrodynamic were insufficient to drag the molecules at the wall if $r_i < R^*$. Assuming the DNA concentration profile to be flat at the entry of a single pore, we deduced that the proportion of molecules escaping from the system during the stacking step was equal to $(R^*/R)^2$. Our model showed that $(R^*/R)^2$ was dependent on the ratio of the transverse to longitudinal migration time, *i.e.*, $\mu_0 E \tau L / R^2$ with τ the viscoelastic fluid relaxation time (Supplementary material). This prediction was in good agreement with the data (dashed line in Fig. 2B). We therefore concluded that high aspect ratio pores were more efficient for DNA retention, and used this film format for the experiments presented hereafter.

Size fractionation of a DNA ladder

We then set out to perform size fractionation by temporally modulating the amplitude of the electric field and hence controlling the amplitude of the transverse migration force. We started with a DNA MW ladder solution composed of 13 bands between 100 and 2000 bp, and used a two-step electric actuation strategy in order to establish that the DNA species could be selectively eluted according to their MW. We applied a maximum tension of 7.5 V for 360 s, followed by a second plateau at 5.5 V for 200 s, and a final step at 0 V for 200 s (Fig. 3A). The corresponding settings in electric field in the pores were 430 and 280 V/cm. The total time of this experiment was ~12.5 min, and the flow rate was set to 240 $\mu\text{L}/\text{min}$, corresponding to a total volume collected at the outlet of 2.7 mL. The DNA solution was initially injected for 2 min (total mass of 97 ng at a concentration of 0.2 ng/ μL) and then rinsed with running buffer for 4 min at the maximum tension. We collected 26 fractions and measured their concentration in time (Fig. 3B). During the first sequence at 7.5 V, the DNA concentration was low (black datasets in Fig. 3B), and the two steps in tension were associated with sudden increases in concentration due to the release of stacked molecules. We then selected the three concentrated fractions indicated by arrows in Fig. 3B to analyze their composition by size separation with the BIABooster technology (see Methods, Fig. 3C). We extracted the mass of each band and normalized them to that of the reference DNA ladder signal (see the analytical workflow in Supplementary Fig. S2) in order to obtain the transfer function of our preparative system. In the high-tension fraction (black dataset), we detected molecules of less than 300 bp at a low concentration because these bands were simply conveyed through the film without any stacking. Conversely, the sample collected upon release of the electric field (blue dataset) was characterized by a high-pass profile with an enrichment in molecules larger than ~800 bp. The composition of the intermediate fraction collected for a tension of 5.5 V corresponded to a band-pass selection filter in the

range of 400 to ~800 bp (red dataset) with a three-fold enrichment of the bands of 400 and 500 bp. Focusing on the collection yield of μ LAF, we considered the two most concentrated fractions for the band-pass and high-pass selected fractions that contained 10 ± 1 and 12 ± 1 ng in 87 and 97 μ L, respectively. We then had to estimate the total mass of DNA conveyed in each step of electric field. For this, we used the size distributions and computed their relative abundance for the mass of each band to match that of the reference ladder. Note that we checked that the size distribution did not change in the fractions collected at each step of pressure (Supplementary Fig. S3). We obtained 26 ± 3 ; 31 ± 3 ; and 41 ± 4 ng in the high-, medium- or low-tension steps, respectively. Therefore, the corresponding collection yields were 32 ± 5 % and 30 ± 5 % in final volumes 5.5 and 4.9-fold reduced as compared to the initial one of 480 μ L, respectively. The corresponding global enrichment factors, defined by the division of the collection yield by the collection to initial volume ratio, were 1.8 and 1.5. In conclusion, these results demonstrated that temporal modulation of the electric field enables us to perform low-pass, band-pass, and high-pass band selection in association to DNA enrichment.

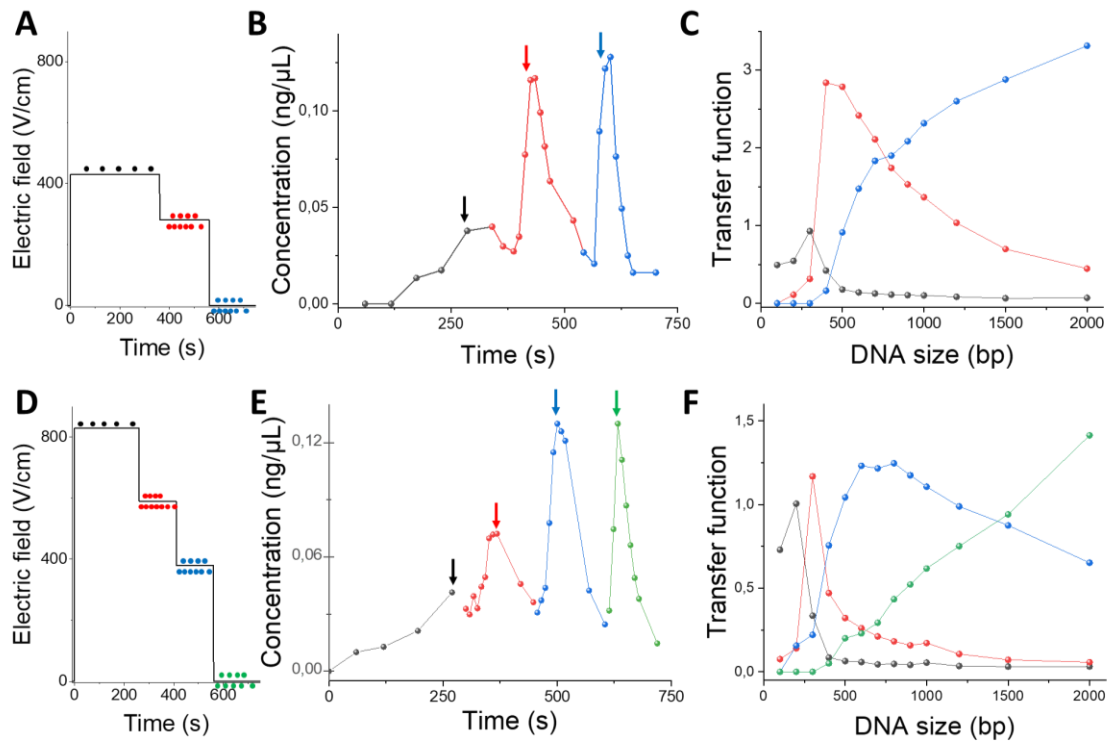


Figure 3: Fractionation of a DNA ladder. (A) Temporal variation of the electric field. The colored dots represent the time points of fraction collection. (B) Total DNA concentration of the collected fractions shown in (A) as a function of time. (C) The DNA concentration normalized to that of the reference ladder sample is plotted as a function of size for the three fractions highlighted by the arrows in panel (B). (D-E-F) Same experiment as in the upper panel with a three-step electric actuation strategy. The flow rate was set to 240 μ L/min in both experiments.

We then investigated whether the DNA ladder sample could be fractionated in multiple outlets by applying three steps in tension of 13, 10 and 7 V, which corresponded to electric fields in the pores of 830, 590, and 380 V/cm, respectively (Fig. 3D). The flow rate was set to 320 $\mu\text{L}/\text{min}$, and the process consisted in injecting the ladder for 120 s (total mass of 160 ng, concentration of 2.5 ng/ μL), followed by four rinsing steps of 150 s at the different electric settings. The total time of this experiment was 12 min, and the processed volume was 3.8 mL. We collected 35 fractions, as indicated by the colored dots in Fig. 2D, and measured their concentration as a function of time (Fig. 3E). We detected three peaks following the drops in tension that were characterized by amplitudes ~ 0.07 ng/ μL for the first one and ~ 0.13 ng/ μL for the second and third ones, as detected in the two-step process. The analysis of the size distribution of the most concentrated fractions indicated by arrows in Fig. 3E showed size fractionation related to a low-pass, two band-pass, and a high-pass filter (Fig. 3F). The first cut-off of the sizes smaller than 200 bp was controlled by an electric field of 830 V/cm (black dataset in Fig. 3F), that was much greater than that in the two-step process of 430 V/cm which produced a low pass filter with a cut-off at 300 bp. The second fraction enabled us to collect the 300 bp fragment with a good selectivity because the concentration of the 200 and 400 bp bands was reduced by a factor of three to four. The collection yield was then be computed by measuring the mass of DNA in peak samples of 12 ± 1 ; 19 ± 2 ; and 13 ± 1 ng in volumes of 166, 152, and 104 μL , respectively. As in the previous experiment, we estimated the mass proportion of the three fractions based on their size distributions, which was equal to 23 ± 2 ; 20 ± 2 ; 90 ± 9 ; and 27 ± 3 ng for the datasets marked with black, red, blue, and green colors in Fig. 3E. Hence, we inferred the collection yield for the red, blue and green samples to be 59 ± 9 ; 21 ± 3 , and $47 \pm 7\%$. Given that the input volume of 640 μL , we deduced the enrichment factor of 2.3, 0.9, and 2.9. Taken collectively, these experiments performed with a DNA ladder proved that μLAF is a versatile fractionation technology with a tunable size selection threshold controlled by the electric field.

Size fractionation of sheared genomic DNA samples

We then wished to apply μLAF to the fractionation of sheared genomic DNA samples (see Methods) with fragment sizes spanning 100 to 2,000 bp (Supplementary Fig. S1B). The original samples, which contained ~ 200 ng of genomic DNA at a concentration of ~ 5 ng/ μL , were diluted at 0.05 ng/ μL in order to obtain an initial volume compatible with multiple operations. We used the same protocol as with the DNA ladder, *i.e.*, we set the flow rate to 230 $\mu\text{L}/\text{min}$ and injected 22 ng of DNA within 2 min. Different electric

actuation temporal sequences were tested with an initial electric field of 560 V/cm then reduced to 270 and 0 V/cm (inset of Fig. 4A), or 530 V/cm followed by 330 V/cm (Fig. 4B, another tension profile is reported in Supplementary Fig. S4). We collected the three fractions of 50 μ L that corresponded to the release of the stacked molecules (instants marked with arrows in the insets). The composition of these samples was then characterized by size separation using the BIABooster, but not with the Qubit fluorimeter because DNA concentration was too low to be detectable. The electropherograms readily confirmed the low-pass, band-pass and high-pass selection (red, blue, and green curves in Fig. 4A-B, respectively), and the possibility to adjust the selection thresholds with the electric field, as detected by e.g., the change of the shape of the green curves. The characterization of the fractionation process was then performed by computing the transfer function to compensate for the uneven size distribution of the input, and the resulting distributions were normalized to unity in order to assess and compare the size selectivity of the three fractions (Fig. 4C). Note that the migration time was converted into DNA size using the reference bands of the ladder which are shown in purple in Fig. 4A-B. We defined the selection thresholds as the sizes at half maximum of the band-pass filter (dark blue curve in Fig. 4C), and measured 370 and 540 bp using electric fields of 530 and 330 V/cm. Note that the size of the peak of the band-pass sample was 436 bp. For the second fractionation process characterized by a step from 560 to 270 V/cm, we obtained thresholds of 390 and 750 bp from the analysis of the light blue curve in Fig. 4C. These measurements of the size thresholds thus confirmed that the selection window could be finely controlled by the electric field in genomic samples.

We then evaluated the collection yields of these processes. For this, we integrated the signal of the band-pass selected samples to determine their mass of 0.24 ± 0.03 and 1.2 ± 0.1 ng for Fig. 4A and 4B, respectively. Given the size selection thresholds of [370-540] bp and [390-750] bp, we computed the corresponding initial inputs based on the integral of the reference signal shown with black dashed lines in Fig. 4A-B, which were equal to 1.25 ± 0.35 and 2.8 ± 0.3 ng. Therefore, the collection efficiency of 19 ± 6 % and 43 ± 8 % was in the same range as in the experiments performed with the DNA ladder. Given the volumes of the collected fraction and initial load of 46 and 460 μ L, respectively, we obtained the corresponding enrichment factors of 1.0 ± 0.3 and 2.2 ± 0.4 . Consequently, μ LAF was readily suited to fractionate genomic DNA samples without significant degradation of the performances in comparison to “ideal” situation of DNA ladders.

While the sample concentration and size distribution are critical for the size selection with silica-based particles, we expected the μ LAF process to be independent of the characteristics of the processed sample. We set out to demonstrate this asset by injecting 2 and 20 ng with two dilutions of the same sample (with the same injection time), and collecting the band-pass fractions for an electric field step of 320 to 260 V/cm. The size distribution of the resulting electropherograms were roughly superposed because the two thick solid blue and two thick red curves, which corresponded to concentrated and diluted inputs, respectively, were comparable (Fig. 4D). Furthermore, the size characteristics of the diluted sample could further be compared to those of the concentrated one by normalizing the data (dotted red curves in Fig. 4D). The four normalized datasets were in good agreement, in turn demonstrating the reproducibility of the selection process. Notably, the latter conclusion was strengthened by assaying the same sample three times consecutively, because the selection thresholds and the peak of the band-pass filter varied by 4% and 5%, respectively (Supplementary Fig. S5).

We also investigated the possibility of narrowing down the size selection window. We performed a set of experiments reducing the amplitude of the jump in the electric field from 560 - 270 V/cm down to 440 - 370, 440 - 400, and 440 - 430 V/cm, and collecting the fraction during the intermediate plateau (blue, cyan, green and red curves in Fig. 4E, respectively). The electrophoregrams showed a marked change from a broad to a peaked response (blue vs. red curves). The size selectivity could then be obtained using the normalized transfer function (Fig. 4F), showing the minimum breadth of 77 bp for a selection window centered at 404 bp. The associated minimum size distribution of 19% was typically twice larger than that of electrophoresis-based technologies⁴, but three times lower than with silica particles⁷.

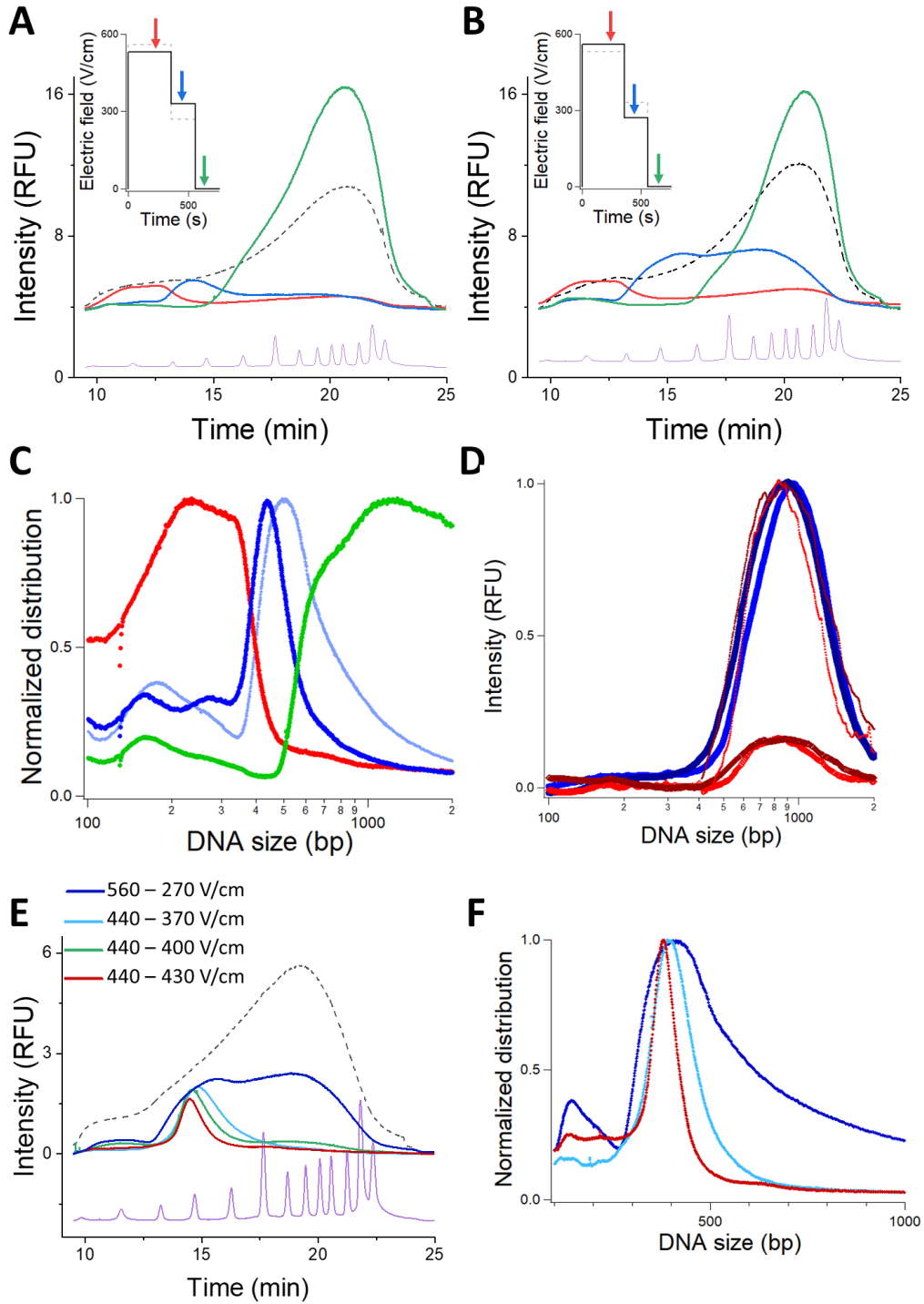


Figure 4: Band-pass fractionation of sheared genomic DNA. (A) Electropherograms of the sheared DNA sample (black dashed curve) and the low-, band-, and high-pass fractions collected at the moments marked with arrows in the inset (red, blue, and green colors, respectively). The purple curve is the electropherogram of the reference ladder. (B) Same as (A) for another scheme of electrical actuation. (C) Normalized transfer functions for the low-, band-, and high-pass selection filters (red, blue, and green curves), as obtained from the data in panel (A). The light blue curve corresponds to the band-pass selected sample for the selection in (B). (D) Intensity vs. size curves obtained with the same sample prepared in two dilutions in order to inject 20 or 2 ng (blue and red datasets, respectively). Note that the process is operated two times consecutively for each initial load. The two thin red curves correspond to the normalization of the thick red ones. (E) Electropherogram of the band-pass fractions as obtained for different steps in the electric field, which are documented in the legend. The black dashed curve is the electropherogram of the input. (F) The curves in (E) are converted into normalized transfer functions with the same colors.

Finally, we tested the possibility of producing multiple fractions in one single round of operation. We loaded 30 ng of sheared DNA at a flow rate of 200 $\mu\text{L}/\text{min}$ and decreased the tension in five consecutive steps of 2 minutes starting from 520 V/cm, then decreasing to 460, 370, 290, and 225 V/cm (inset of Fig. 5A, the total duration of the experiment is set to 16 minutes). The characterization of the resulting six fractions by the BIABooster showed a progressive shift from the low to high MW range (Fig. 5A). By computing the normalized transfer functions, we proved that the initial sample had been partitioned into a low-pass, four band-pass, and one high-pass samples (Fig. 5B). Their respective selection thresholds were <282, 188-350, 331-489, 382-700, 473-1547, and >925 bp. We focused on the four band-pass filtered samples, and determined their respective mass of DNA by integration of the electrophoregrams, which were 0.38 \pm 0.08; 0.51 \pm 0.10; 0.81 \pm 0.16; and 1.56 \pm 0.31 ng. By integration of the input genomic signal in between the thresholds of each filtered samples, we could infer the collection yields of 20 \pm 6, 33 \pm 9, 31 \pm 9, 10 \pm 3%, respectively. Moreover, given that the collection volume was 50 μL for an injection of 600 μL , we deduced the enrichment factors of 2.2 \pm 0.7, 3.8 \pm 1.1, 3.5 \pm 1.1, 1.2 \pm 0.3. These characteristics, which were obtained with five steps in the electric field, were consistent to those obtained with single- or two-step selection, showing the versatility and performance of μLAF .

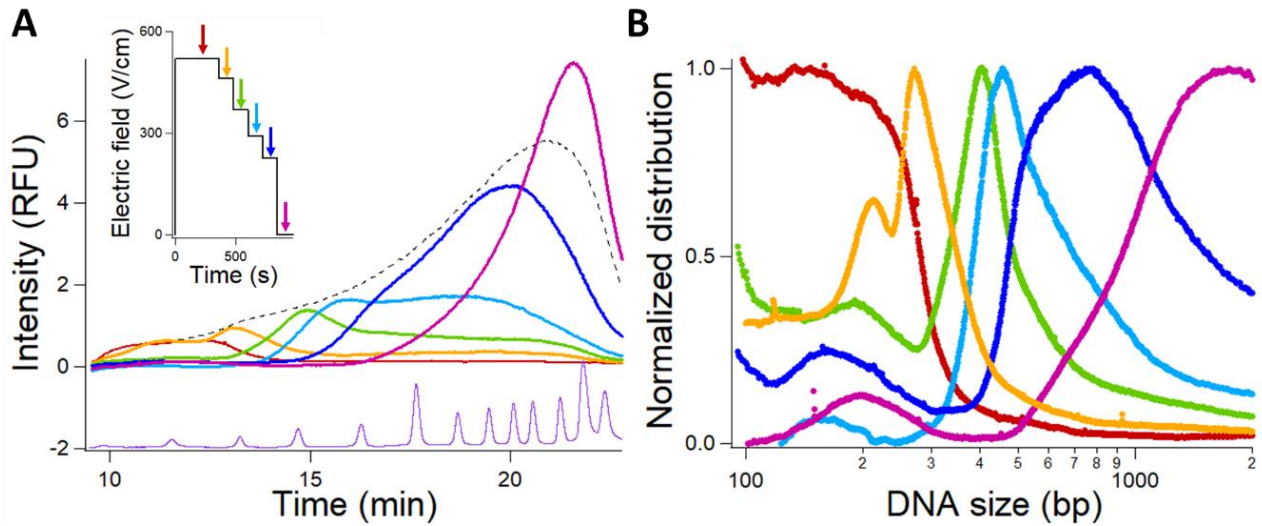


Figure 5: Sampling sheared genomic DNA into multiple fractions. (A) Electropherograms of sheared genomic DNA (black dashed curve) and the six fractions collected during the selection process. The inset shows the temporal profile of the electric field, and the arrows indicate the collection times. (B) Normalized transfer functions of the six fractions shown in (A) using the same colors.

Discussion

We presented and optimized the μ LAF technology to perform the size fractionation of genomic DNA samples. We demonstrated its performance for fractionation in the range of 200 to 2000 bp, collecting up to six fractions from a broadly-distributed input. The whole process, which took 10 to 20 minutes, enabled the fractionation of ~ 0.5 mL samples into 50 μ L outlets. The mass of the input that ranged from a few ng to several hundreds of ng did not interfere with the selection process for the size thresholds were controlled by the electric field. In addition to these performances, we point out that the operation of μ LAF only required a pressure generator of ~ 1 bar and a DC power supply of ~ 10 V, *i.e.*, broadly-accessible equipments. Future developments for the μ LAF technology include the enhancement of the collection yield to more than 50%, keeping the collection volume to 50 μ L. This task requires the minimization of the dispersion during the collection step because the convection to the outlet is associated to Taylor dispersion²⁶. Reducing Taylor dispersion can be achieved by shortening the lag time of ~ 100 s between the drop in electric field and the collection of the outlet (see e.g., Fig. 2A). We suggest to optimize the geometry of the outlet channel by reducing its volume, and hence its flushing time. In the longer term, we propose to integrate the function of purification, *i.e.*, salt and/or protein removal, in the process flow. At the level of a single capillary, this integration of functions was successfully demonstrated with the μ LAS technology for the direct analysis of cell-free DNA in blood plasma²⁷. Using isopore films, this objective nevertheless raises several challenges because the presence of salt in the buffer is associated with (i) an onset in electric current during the operation, and (ii) a decrease of the dielectric permittivity with salt concentration that reduces the electric field in the pores during purification. These constraints are mutually-reinforcing, because the change in permittivity is compensated with an increased electric field, which creates more current. In turn, this example demonstrates that engineering models to predict the function of μ LAF would constitute an asset for future developments and for optimization of its performances.

Acknowledgements. We are thankful to Audrey Boutonnet, Frédéric Ginot, Audrey Cochard, Gwenaël Bonfante for critical reading of the manuscript, and Jeffrey Teillet for technical support in LabView automation. We

thank the support of the MultiFab platform for stereolithography. This project was supported by the FEDER project “PURE-Tech” and by the “Biology and Basic Sciences for Cancer research” fund of the INCa (project PLBIO).

Bibliography

- (1) Tan, S. C.; Yiap, B. C. DNA, RNA, and Protein Extraction: The Past and The Present. *Journal of Biomedicine and Biotechnology* **2009**, 2009, 1–10. <https://doi.org/10.1155/2009/574398>.
- (2) J Shetty, P. The Evolution of DNA Extraction Methods. *AJBSR* **2020**, 8 (1), 39–45. <https://doi.org/10.34297/AJBSR.2020.08.001234>.
- (3) Duro, G.; Izzo, V.; Barbieri, R. Methods for Recovering Nucleic Acid Fragments from Agarose Gels. *J Chromatogr* **1993**, 618 (1–2), 95–104. [https://doi.org/10.1016/0378-4347\(93\)80029-4](https://doi.org/10.1016/0378-4347(93)80029-4).
- (4) Quail, M. A.; Gu, Y.; Swerdlow, H.; Mayho, M. Evaluation and Optimisation of Preparative Semi-Automated Electrophoresis Systems for Illumina Library Preparation. *Electrophoresis* **2012**, 33 (23), 3521–3528.
- (5) Smerkova, K.; Dostalova, S.; Vaculovicova, M.; Kynicky, J.; Trnkova, L.; Kralik, M.; Adam, V.; Hubalek, J.; Provaznik, I.; Kizek, R. Investigation of Interaction between Magnetic Silica Particles and Lambda Phage DNA Fragment. *Journal of Pharmaceutical and Biomedical Analysis* **2013**, 86, 65–72. <https://doi.org/10.1016/j.jpba.2013.07.039>.
- (6) McCormick, R. M. A Solid-Phase Extraction Procedure for DNA Purification. *Analytical Biochemistry* **1989**, 181 (1), 66–74. [https://doi.org/10.1016/0003-2697\(89\)90394-1](https://doi.org/10.1016/0003-2697(89)90394-1).
- (7) Quail, M. A.; Swerdlow, H.; Turner, D. J. Improved Protocols for the Illumina Genome Analyzer Sequencing System. *CP Human Genetics* **2009**, 62 (1). <https://doi.org/10.1002/0471142905.hg1802s62>.
- (8) Berensmeier, S. Magnetic Particles for the Separation and Purification of Nucleic Acids. *Appl Microbiol Biotechnol* **2006**, 73 (3), 495–504. <https://doi.org/10.1007/s00253-006-0675-0>.
- (9) Irie, T.; Oshida, T.; Hasegawa, H.; Matsuoka, Y.; Li, T.; Oya, Y.; Tanaka, T.; Tsujimoto, G.; Kambara, H. Automated DNA Fragment Collection by Capillary Array Gel Electrophoresis in Search of Differentially Expressed Genes. *Electrophoresis* **2000**, 21 (2), 367–374. [https://doi.org/10.1002/\(SICI\)1522-2683\(20000101\)21:2<367::AID-ELPS367>3.0.CO;2-1](https://doi.org/10.1002/(SICI)1522-2683(20000101)21:2<367::AID-ELPS367>3.0.CO;2-1).
- (10) Minarik, M.; Klepárník, K.; Gilár, M.; Foret, F.; Miller, A. W.; Sosic, Z.; Karger, B. L. Design of a Fraction Collector for Capillary Array Electrophoresis. *Electrophoresis* **2002**, 23 (1), 35. [https://doi.org/10.1002/1522-2683\(200201\)23:1<35::AID-ELPS35>3.0.CO;2-H](https://doi.org/10.1002/1522-2683(200201)23:1<35::AID-ELPS35>3.0.CO;2-H).
- (11) Muller, Odilo.; Foret, Frantisek.; Karger, B. L. Design of a High-Precision Fraction Collector for Capillary Electrophoresis. *Anal. Chem.* **1995**, 67 (17), 2974–2980. <https://doi.org/10.1021/ac00113a036>.
- (12) Khandurina, J.; Guttman, A. Micromachined Capillary Cross-Connector for High-Precision Fraction Collection. *Journal of Chromatography A* **2002**, 979 (1–2), 105–113. [https://doi.org/10.1016/S0021-9673\(02\)01261-X](https://doi.org/10.1016/S0021-9673(02)01261-X).
- (13) Sun, K.; Li, Z.; Ueno, K.; Juodkazis, S.; Noji, S.; Misawa, H. Electrophoretic Chip for High-Fidelity Fractionation of Double-Stranded DNA. *Electrophoresis* **2007**, 28 (10), 1572–1578. <https://doi.org/10.1002/elps.200600685>.
- (14) Lin, R.; Burke, D. T.; Burns, M. A. Addressable Electric Fields for Size-Fractionated Sample Extraction in Microfluidic Devices. *Anal. Chem.* **2005**, 77 (14), 4338–4347. <https://doi.org/10.1021/ac048132o>.
- (15) Gumuscu, B.; Bomer, J. G.; De Boer, H. L.; Van Den Berg, A.; Eijkel, J. C. Exploiting Biased Reptation for Continuous Flow Preparative DNA Fractionation in a Versatile Microfluidic Platform. *Microsystems & Nanoengineering* **2017**, 3, 17001.
- (16) Huang, L. R.; Tegenfeldt, J. O.; Kraeft, J. J.; Sturm, J. C.; Austin, R. H.; Cox, E. C. A DNA Prism for High-Speed Continuous Fractionation of Large DNA Molecules. *Nat Biotech* **2002**, 20 (10), 1048–1051. <https://doi.org/10.1038/nbt733>.

- (17) Feng Cheow, L.; Bow, H.; Han, J. Continuous-Flow Biomolecule Concentration and Detection in a Slanted Nanofilter Array. *Lab Chip* **2012**, *12* (21), 4441. <https://doi.org/10.1039/c2lc40195a>.
- (18) Andriamanampisoa, C.-L.; Bancaud, A.; Boutonnet-Rodat, A.; Didelot, A.; Fabre, J.; Fina, F.; Garlan, F.; Garrigou, S.; Gaudy, C.; Ginot, F. BIABooster: Online DNA Concentration and Size Profiling with a Limit of Detection of 10 Fg/ML and Application to High-Sensitivity Characterization of Circulating Cell-Free DNA. *Analytical chemistry* **2018**, *90* (6), 3766–3774.
- (19) Ranchon, H.; Malbec, R.; Picot, V.; Boutonnet, A.; Terrapanich, P.; Joseph, P.; Leïchl  , T.; Bancaud, A. DNA Separation and Enrichment Using Electro-Hydrodynamic Bidirectional Flows in Viscoelastic Liquids. *Lab Chip* **2016**, *16* (7), 1243–1253. <https://doi.org/10.1039/c5lc01465d>.
- (20) Chami, B.; Socol, M.; Manghi, M.; Bancaud, A. Modeling of DNA Transport in Viscoelastic Electro-Hydrodynamic Flows for Enhanced Size Separation. *Soft matter* **2018**, *14* (24), 5069–5079.
- (21) Arca, M.; Butler, J. E.; Ladd, A. J. Transverse Migration of Polyelectrolytes in Microfluidic Channels Induced by Combined Shear and Electric Fields. *Soft matter* **2015**, *11* (22), 4375–4382.
- (22) Butler, J. E.; Usta, O. B.; Kekre, R.; Ladd, A. J. C. Kinetic Theory of a Confined Polymer Driven by an External Force and Pressure-Driven Flow. *Physics of Fluids* **2007**, *19*, 113101.
- (23) Milon, N.; Chantry-Darmon, C.; Satge, C.; Fustier, M.-A.; Cauet, S.; Moreau, S.; Callot, C.; Bellec, A.; Gabrieli, T.; Sa  as, L. MLAS Technology for DNA Isolation Coupled to Cas9-Assisted Targeting for Sequencing and Assembly of a 30 Kb Region in Plant Genome. *Nucleic acids research* **2019**, *47* (15), 8050–8060.
- (24) Tijunelyte, I.; Malbec, R.; Chami, B.; Cacheux, J.; Dez, C.; Leïchl  , T.; Cordelier, P.; Bancaud, A. Micro-RNA 21 Detection with a Limit of 2 PM in 1 Min Using a Size-Accordable Concentration Module Operated by Electrohydrodynamic Actuation. *Biosensors and Bioelectronics* **2021**, *178*, 112992. <https://doi.org/10.1016/j.bios.2021.112992>.
- (25) Milon, N.; Fuentes Rojas, J.-L.; Castinel, A.; Bigot, L.; Bouwmans, G.; Baudelle, K.; Boutonnet, A.; Gibert, A.; Bouchez, O.; Donnadi  u, C.; Ginot, F.; Bancaud, A. A Tunable Filter for High Molecular Weight DNA Selection and Linked-Read Sequencing. *Lab Chip* **2020**, *20* (1), 175–184. <https://doi.org/10.1039/c9lc00965e>.
- (26) Teillet, J.; Martinez, Q.; Tijunelyte, I.; Chami, B.; Bancaud, A. Characterization and Minimization of Band Broadening in DNA Electrohydrodynamic Migration for Enhanced Size Separation. *Soft Matter* **2020**, *16* (24), 5640–5649. <https://doi.org/10.1039/D0SM00475H>.
- (27) Boutonnet, A.; Pradines, A.; Mano, M.; Kreczman-Brun, M.; Mazi  res, J.; Favre, G.; Ginot, F. Size and Concentration of Cell-Free DNA Measured Directly from Blood Plasma, without Prior DNA Extraction. *Anal. Chem.* **2023**, *95* (24), 9263–9270. <https://doi.org/10.1021/acs.analchem.3c00998>.
- (28) Feynman, R. P.; Leighton, R. B.; Sands, M. L. *The Feynman Lectures on Physics. 2: Mainly Electromagnetism and Matter*, 6. print., commemorative issue.; Addison-Wesley: Reading, Mass, 1995.
- (29) Chami, B.; Socol, M.; Manghi, M.; Bancaud, A. Modeling of DNA Transport in Viscoelastic Electro-Hydrodynamic Flows for Enhanced Size Separation. *Soft Matter* **2018**, *14* (24), 5069–5079. <https://doi.org/10.1039/c8sm00611c>.
- (30) Naillon, A.; de Loubens, C.; Ch  vremont, W.; Rouze, S.; Leonetti, M.; Bodiguel, H. Dynamics of Particle Migration in Confined Viscoelastic Poiseuille Flows. *Phys. Rev. Fluids* **2019**, *4* (5), 053301. <https://doi.org/10.1103/PhysRevFluids.4.053301>.

SUPPLEMENTARY MATERIAL

SIZE-FRACTIONATION OF MILLI-LITER DNA SAMPLES IN MINUTES CONTROLLED BY AN ELECTRIC FIELD OF ~10 V

Paul Bruand^{1,2}, Inga Tijunelyte¹, Adrien Castinel³, Cécile Donnadiou³, Pierre Joseph¹, Aurélien Bancaud^{1,*}

¹*CNRS, LAAS, 7 avenue du colonel Roche, F-31400, Toulouse, France.*

²*Adelis, 478 Rue de la Découverte, 31670 Labège, France*

³*GeT-PlaGe, US 1426, Genotoul, INRAE, 31320 Castanet-Tolosan, France*

Guidelines for the conception of the electrodes

We present the calculation of the electric potential function of the charged electrodes using the Feynman lectures on Physics²⁸. Using a 2D geometry and describing the electrode regular mesh with a characteristic distance a between the wires, we aim to determine the potential $\phi(x, z)$ with z the axis parallel to the fluid flow direction and x the perpendicular axis. The electric potential function in this case can be written as a harmonic function, *i.e.*, the sum of several harmonic sub-functions of the form:

$$\phi_n(x, z) = F_n(z) \cos \frac{2\pi nx}{a} \quad (1)$$

where n is the rank of the harmonic. The harmonic of rank 0 does not depend on x ; it is the uniform component. The higher harmonics are sinusoidal according to x . Solving Laplace equation leads to

$$F_n(z) = A_n e^{-2\pi n z/a} \quad (2)$$

If we place the isopore film at a distance of 2 mm, *i.e.*, four times the electrode grid size a of 500 μm , the first harmonic has a negligible amplitude due to the exponential dependence in z .

The electric field inside the pores of the film can be expressed as:

$$E = \frac{\Delta U}{d + 2L\pi r^2/S^2} \quad (3)$$

With ΔU the applied tension, d the thickness of the film, L the distance between the film and one electrode (2 mm), r the pore size, S the working section of the film.

The mean hydrodynamic speed can be expressed as:

$$v_{hydro} = \frac{\varphi r^2 \Delta P}{8\eta d} \quad (4)$$

With φ the porosity of the film, ΔP the applied pressure, η the viscosity of the solution.

Experimentally, these two parameters are deduced from the following formula:

$$E_{exp} = \frac{\rho}{d} \left(\frac{2L}{S} + \frac{d}{S\varphi} \right) I_{exp} \quad (5)$$

With ρ the measured resistivity of the solution, and I_{exp} the current measured.

$$v_{hydro\ exp} = \frac{Q_{exp}}{nS} \quad (6)$$

With Q_{exp} the measured flow.

Model of DNA escape from the concentration module

We reported an analytical expression of the transverse viscoelastic force²⁹:

$$F_T(r) = 16\pi K \tau \eta a v_{h0} v_e \frac{r}{R^2} \quad (7)$$

with r the radial position in the channel, K a constant, τ the characteristic time of the viscoelastic fluid, η the fluid viscosity, a hydrodynamic radius of the DNA, v_{h0} the maximum hydrodynamic velocity, v_e the electrophoretic velocity, and R the radius of the pore. Transverse migration is the result of the balance between this transverse force and Stokes drag force assuming a typical size of the DNA.

$$F_T(r) = 6\pi\eta a \frac{dr}{dt} \quad (8)$$

The Péclet number ($P_{e_M} = Rv_{h0}/D$ with $D = k_B T / 6\pi\eta a$ the diffusion coefficient) is on the order of $P_{e_M} \sim 10^5 \gg 1$ given that $R=1 \mu\text{m}$, $v_{h0}=10^{-2} \text{ m/s}$, and $D=10^{-13} \text{ m}^2/\text{s}$. Hence, convection is dominant over diffusion. Hence, transverse migration can be modelled with a first order differential equation:

$$\frac{dr}{dt} = \frac{8}{3} K \tau v_{h0} v_e \frac{1}{R^2} r \quad (9)$$

We hereafter denote $\alpha = 8K\tau v_{h0} v_e / 3R^2$, as the inverse of characteristic time scale for the transverse migration. The migration along the pore is dictated by the following equation:

$$\frac{dz}{dt} = v_{h0} \left(1 - \frac{r(t)^2}{R^2} \right) - v_e \quad (10)$$

Using the solution of Eq. (7) for an initial position r_i at the entry of the pore, we can integrate Eq. (8):

$$z(t) = (v_{h0} - v_e)t - \frac{r_i^2}{R^2} \frac{v_{h0}}{2\alpha} (e^{2\alpha t} - 1) \quad (11)$$

Injecting the solution of Eq. (7), we deduce a parametric equation for the migration distance as a function of the radial position r of the molecule:

$$z(r) = \frac{v_{h0} - v_e}{\alpha} \ln\left(\frac{r}{r_i}\right) - \frac{v_{h0}}{2\alpha} \left(\frac{r^2 - r_i^2}{R^2} \right) \quad (12)$$

the molecule is arrested if transverse forces convey it at the vicinity of the walls where electrophoresis is predominant, equivalently $z(R) < L$ with L the length of pore. We can then write

$$L = \frac{v_{h0} - v_e}{\alpha} \ln\left(\frac{R}{R^*}\right) - \frac{v_{h0}}{2\alpha} \left(1 - \frac{R^{*2}}{R^2} \right) \quad (13)$$

If we consider a uniform distribution of DNA over the cross-section of the pore at its entrance, we can define the DNA leakage Φ as the ratio of the cross-section corresponding to the lost DNA to the total cross-section of the pore:

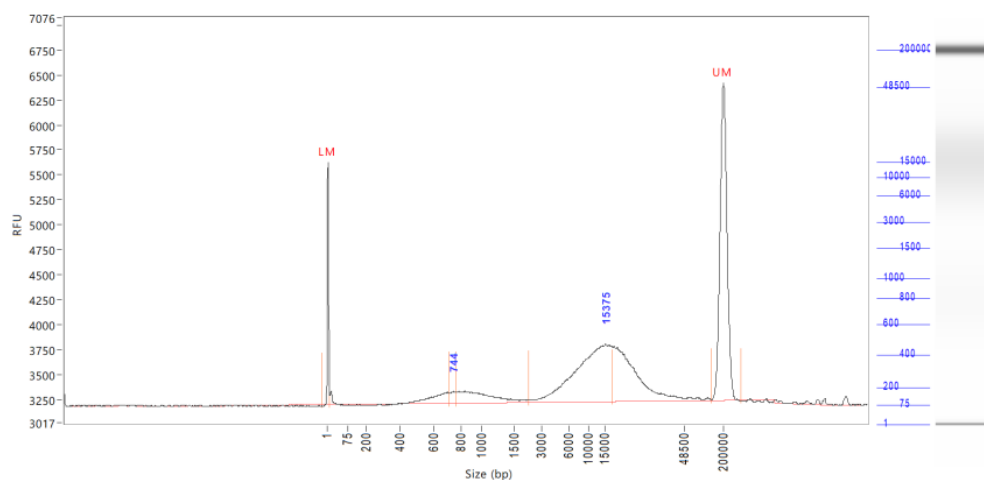
$$\Phi = \frac{R^{*2}}{R^2} \quad (14)$$

This expression can be simplified, once we consider $v_{h0} \gg v_e$ (in our experimental conditions, we have $v_{h0} > 20v_e$):

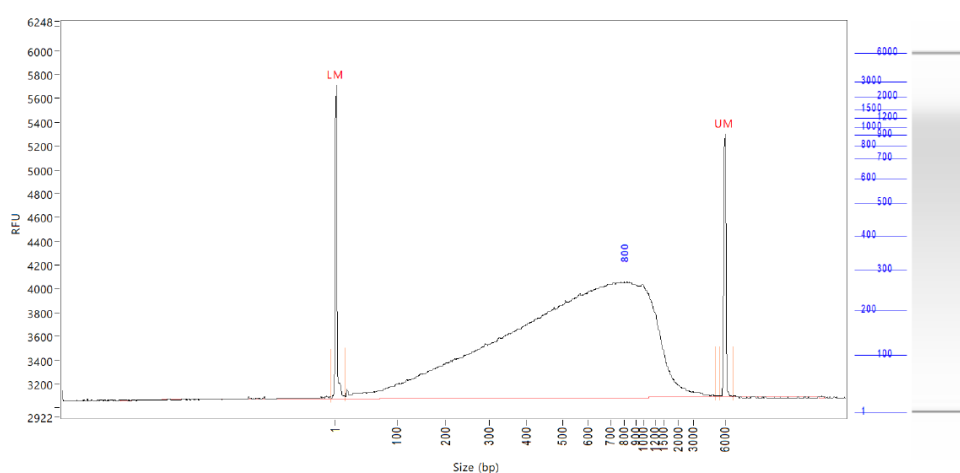
$$L \sim \frac{-3R^2}{16K\tau v_e} [1 - \Phi + \ln(\Phi)] \quad (15)$$

Taking $\tau = 2 \text{ ms}$ for the fluid viscoelastic time³⁰, the fit value of K obtained from the data in Fig. 2B is $1.4 \cdot 10^{-3}$. The prefactor is qualitatively explained by the ratio of the transverse migration time $1/\alpha$ with the longitudinal migration time of v_{h0}/H .

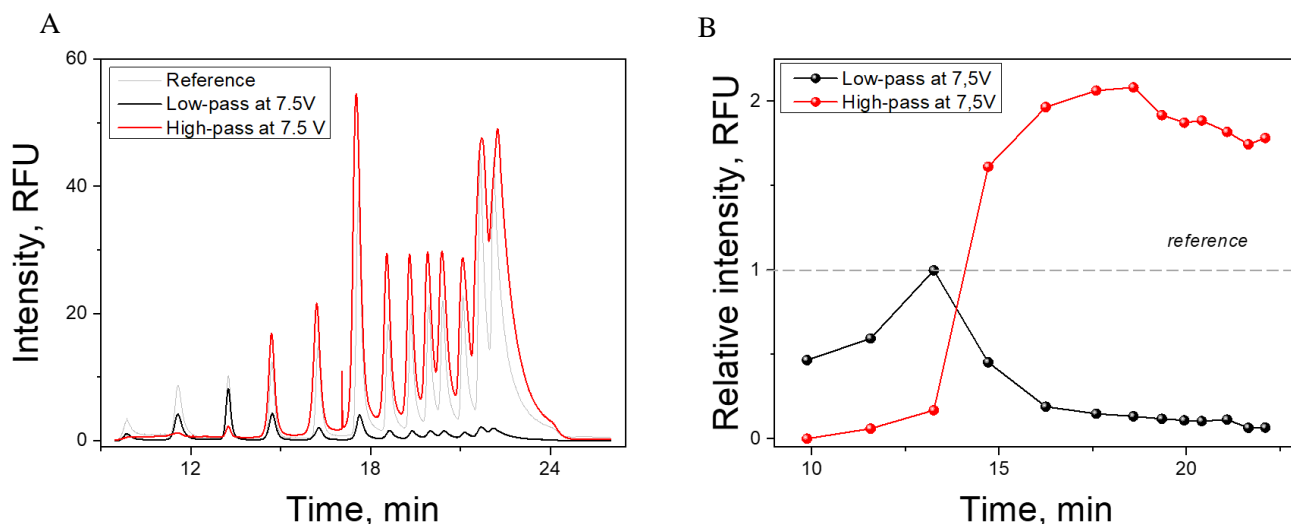
A Sample: 41393
Well Location: G2
Created: Tuesday, August 23, 2022 4:51:55 PM



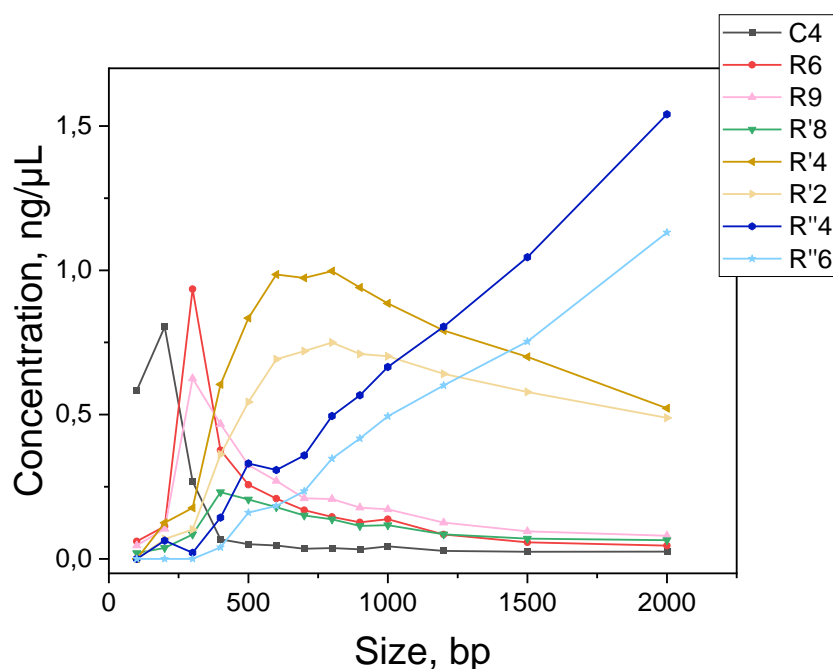
B Sample: 41393-2
Well Location: A2
Created: Tuesday, October 4, 2022 5:36:42 PM



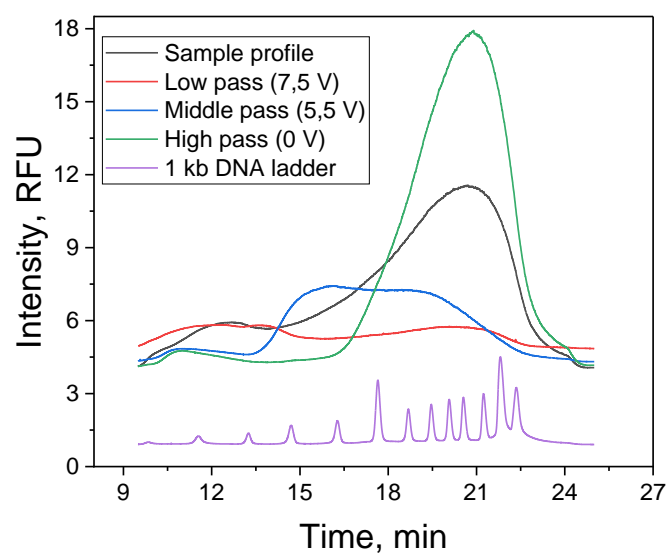
Supplementary Fig. S1: Genomic sample characterization with the Fragment Analyzer. (A) Genomic DNA as obtained after the extraction protocol. **(B)** Same sample after mechanical shearing.



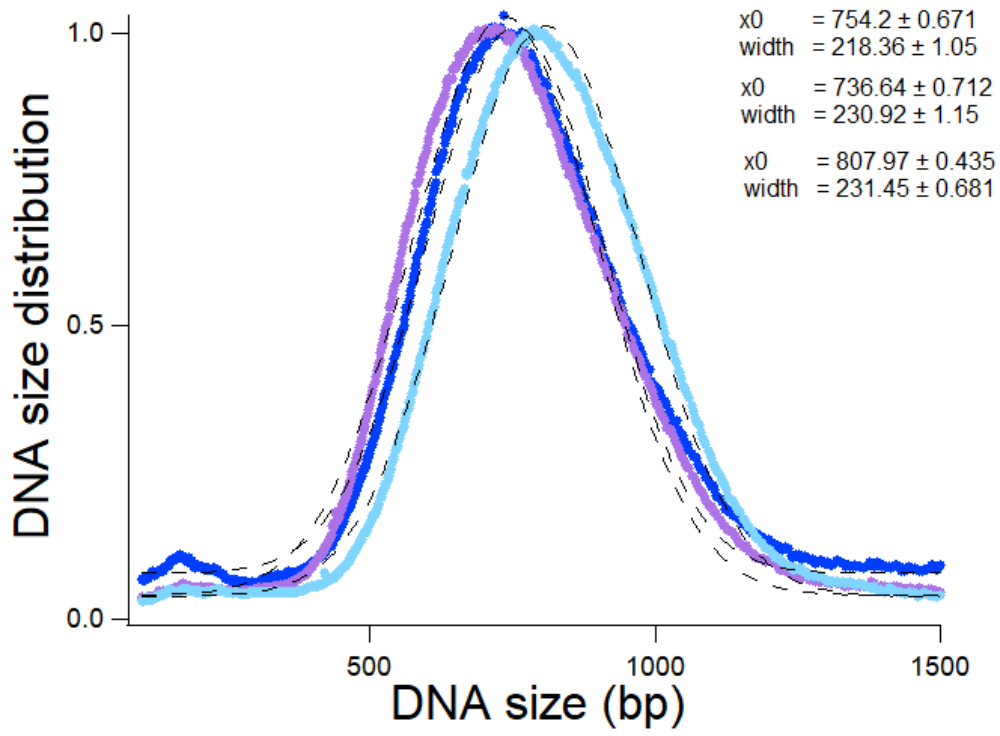
Supplementary Fig. S2: Conversion of electrophoregrams into concentration vs. size plots. (A) The gray curve represents the electrophoregram of the 100 bp DNA ladder as obtained with the BIABooster. The black and red curves show the samples collected during the stacking steps and after the release of the electric field, denoted “low-pass” and “high-pass”, respectively. (B) After integration of the different bands using a Gaussian fit model and normalizing this response to that of the reference, we report the relative intensity of each band as a function of time. Note that the migration time and DNA size can be unambiguously assigned.



Supplementary Fig. S3: Composition of different fractions collected during the sampling process. The graph shows the concentration of different fractions as a function of size for the experiment shown in Fig. 3D-E-F in main text. For the three steps in tension, we analyze the most concentrated fractions (shown with strong colors) and one more diluted fraction after 60 s in the corresponding light colors. This data shows that the global concentration decreases but the size distribution remains roughly constant during the steps in tension.



Supplementary Fig. S4: Electropherograms for the same operation as Fig. 4A-B but different electric field settings. The black curve is the input genomic DNA, and the low-, band-, and high-pass fractions are shown in red, blue, and green colors, respectively. The purple curve is the electropherogram of the reference ladder. The electric field was set to 412 and 270 V/cm for actuation tension of 7.5 and 5.5 V, respectively.



Supplementary Fig. S5: Triplicate DNA size selection. The cyan, purple and blue electrophoregrams show three band-pass selected samples obtained consecutively from the same input with a two-step electrical actuation scheme characterized by 320 to 260 V/cm. The three black dashed curves are the corresponding Gaussian fits. The three peaks and widths are reported in the legend.